

Exploratory Study of Conductivity in Detonation Waves

F. K. Lu,^{*} C. H. Kim,[†] D. R. Wilson,[‡] H.-C. Liu,[§] and W. S. Stuessy^{**}

University of Texas at Arlington, Arlington, Texas 76019-0018

G. A. Simmons^{††}

MSE-TA, Inc., Butte, MT 59702

Shock tube experiments were performed to measure the conductivity of the plasma of detonation products for potential applications in hybrid pulse detonation engines. Detonations of hydrogen/oxygen, hydrogen/air and propane/oxygen established Chapman-Jouguet shocks. The experiments indicated that seed such as potassium carbonate did not appear to significantly increase the conductivity over the unseeded gases. The conductivity measurements were compared against values obtained assuming chemical equilibrium and found to be quite small. The reasons for this anomalous behavior were attributed to incomplete mixing of the reactants and non-uniform seed distribution.

Introduction

RECENT technology developments are making it feasible for advanced propulsion concepts to be applied to hypersonic flight in the earth's atmosphere and also for interplanetary travel.¹ One such concept involves the use of high pressure, magnetohydrodynamic (MHD) accelerators with a pulse detonation engine (PDE). Alternatively, MHD generators have been proposed to operate with PDEs. Before such MHD devices can be implemented, a better understanding of the process that couples the electromagnetic field to the high enthalpy, high-pressure gas is crucial, particularly when operated in a pulsed environment. Typical MHD devices rely on a continuous, uniform flow of plasma through externally applied electric and magnetic fields. For good efficiency and performance of MHD accelerators, the plasma must be highly conductive. The PDE exhaust, unfortunately, does not produce sufficient conductivity. To enhance the conductivity of the gas, a pre-ionization scheme may be needed by mixing the gas with a seed material that has low ionization potential. Examples of such materials are

potassium or cesium salts.

To develop an understanding of the conductivity of high-pressure plasmas in a pulsed mode, single-shot experiments were performed using a detonation-driven shock tube, a technique for generating high-enthalpy flows first proposed by Bird.² The detonation process has been successfully used as an inexpensive, simple and viable alternative to free-piston drivers for obtaining high-enthalpy flows.³ The detonation is established in a tube filled with a near-stoichiometric oxyhydrogen mixture, although other gas combinations are possible, such as acetylene and oxygen.⁴ The detonation-driven shock tube can yield a single pulse of high-enthalpy flows at PDE exhaust conditions. This provides a simple means of simulating the actual continuous pulsating flow in a PDE.

Previous experiments of aerodynamic plasmas have been reported in Refs. 5 and 6. These studies were at pressures of a few atmospheres. Results from those early investigations are not directly pertinent to combustion applications at higher pressure. Experiments were recently performed to explore the conductivity of weakly ionized plasmas generated from gaseous detonation products seeded with a small amount of alkali salt. The experiments made use of a facility used previously to study the conductivity of high-enthalpy, seeded air plasmas.⁷

In the reported experiments, the driver tube was filled with combinations of gaseous fuel, such as hydrogen and propane, and oxidizer, such as oxygen and air. The mixture was seeded with potassium carbonate. The gases were initially at room temperature. However, by varying the mixture pressure, different end states of detonation were achieved. This detonated gas passed through a test section that enabled the average conductivity to be measured.

This paper summarizes the experimental study. The

^{*}Professor, Mechanical and Aerospace Engineering Department, and Director, Aerodynamics Research Center. Associate Fellow AIAA.

[†]Graduate Teaching Assistant, Aerodynamics Research Center, Mechanical and Aerospace Engineering Department. Student Member AIAA.

[‡]Professor and Chair, Mechanical and Aerospace Engineering Department. Associate Fellow AIAA.

[§]Graduate Research Associate, Aerodynamics Research Center, Mechanical and Aerospace Engineering Department; presently, Institute of Aeronautics and Astronautics, National Cheng Kung University, Tainan, Taiwan. Student Member AIAA.

^{**}Research Associate, Aerodynamics Research Center, Mechanical and Aerospace Engineering Department. Senior Member AIAA.

^{††}Engineer. Advance Energy & Aerospace Programs. Senior Member AIAA.

experimental results were compared against those predicted by the NASA CEA chemical equilibrium code.⁸ The experimental conductivity was found to be considerably smaller than those obtained with CEA for all mixtures. The discrepancy between experiment and theory was thought to be due to incomplete mixing of the reactants and non-uniform seed distribution. Nevertheless, the experiments indicated ways for improving seed injection systems in a pulsed mode.

Experimental Technique

Facility

A high-performance, detonation-driven shock tube was used to generate the test flow.⁹ The shock tube consists of a high-pressure tube, a detonation tube and a driven tube as shown schematically in Fig. 1(a). This facility can produce static pressures of up to 34 atm and static temperatures of up to 4200 K.

The driver tube was filled with either air or helium and was used to induce a detonation wave in the detonation tube. The driver tube had a bore of 152.4 mm (6 in.) and a length of 3 m (10 ft). The detonation tube also had a bore of 152.4 mm (6 in.) but was 2.74 m (9 ft) long. Both tube sections were rated for a pressure of 41.3 MPa (6000 psi). These two tubes were separated by a 114 mm (4.5 in.) double diaphragm section. The diaphragms were usually constructed from 3.42 or 2.66 mm (10 or 12 gauge) hot-rolled 1008 steel plates, scored to various depths in a cross pattern. A thin Mylar diaphragm separated the detonation and driven tubes. The driven tube had a bore of 41.25 mm (1.624 in.) and a length of over 9 m (30 ft), and it was open to the atmosphere. It was made of type 304 stainless steel with a pressure rating of 19 MPa (2800 psi). The driver-to-driven tube area ratio was 13.7, which yielded an improvement in performance. A conductivity channel was mounted at the downstream end of the driven tube. Another section of tube, 6.12 m (20.1 ft) long, was installed downstream of the conductivity channel to prevent wave reflections from the open end from interfering with the test flow.

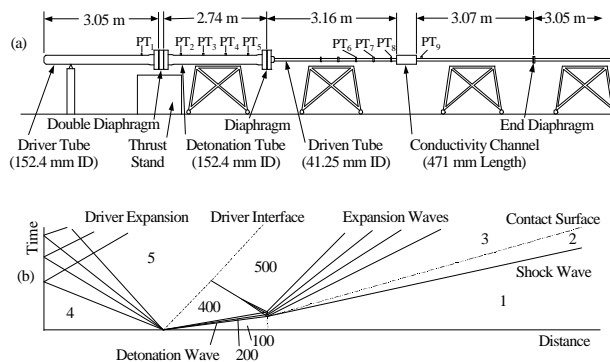


Figure 1. (a) Schematic of the UTA detonation-driven shock tube. (b) Simplified wave diagram for given tube geometry.

Instrumentation

The detonation tube was instrumented with four flush-mounted PCB model 111A22 dynamic pressure transducers, as indicated in Fig. 1(a), and a MKS model 127A Baratron pressure transducer. The Baratron transducer had a maximum pressure range of 1.33 MPa (193 psi), and was used to set the mixture ratio when filling the detonation driver. The Baratron pressure transducer was also used to provide an initial pressure reading for the PCB transducers. The PCB transducers had a full-scale range of 68.9 MPa (10,000 psi), rise time of 2 μ s, and a time constant of 1000 s. Their locations relative to the double diaphragm were 0.50, 1.08, 1.66, and 2.25 m, respectively.

The driven tube was instrumented by four PCB model 111A23 transducers. Two model 111A23 transducers, with a full-scale pressure range of 34.4 MPa (5000 psi), rise time of 2 μ s, and a time constant of 500 s, were located upstream of the test section and were used primarily for shock speed determination. The two other PCB transducers were either model 111A23 or 111A24, depending upon the conditions in the driven tube. Model 111A24 transducers had a full-scale range of 6.89 MPa (1000 psi), a response time of 2 μ s, and a time constant of 100 s. A MKS model 127A Baratron pressure transducer was used to measure the initial pressure in the driven tube. This transducer had a maximum pressure range of 133 kPa (19 psi). It provided an accurate measurement of the initial pressure in the driven tube as well as serving to initialize the dynamic PCB transducers.

Conductivity Channel and Power Supply

Electrical conductivity was measured in a channel connected to the end of the driven section. The conductivity measurement channel consisted of a pair of powered electrodes and 20 probe electrodes separated by insulators.¹⁰ The powered electrodes provided an axial electrical field obtained by discharging a capacitor bank. The electrodes were made of oxygen-free copper with an electrical resistivity of 1.69 $\mu\Omega$ ·cm at 300 K. The electrodes had the same inside diameters as the driven tube and had outside diameters of 139.7 mm (5.5 in.). The 20 electrodes had thicknesses of 3.18 mm (0.125 in.) and were used for measuring the voltage drop along the channel. Insulator rings with the same radial dimensions were made from 1.59 mm (0.0625 in.) thick Teflon. The total length of the measurement channel, including the powered electrodes, the probe electrodes and the insulators, was 115.9 mm (4.563 in.). The channel dimensions were used to size the power supply as described in Ref. 10. Lexan tubes of 152.4 mm (6 in.) length were mounted on both ends of the conductivity channel to isolate it electrically from the shock tube. As will be subsequently described, the voltage gradient across the 20 probe electrodes was fairly uniform. Thus, the

channel yielded a radially averaged conductivity measurement.

A capacitor bank, with inductors arranged in a pulse-forming network, delivered the potential across the plasma.¹¹ It was designed for a maximum charge voltage of 8 kV. The design of the electrode power supply required an estimate of the voltages and currents for the anticipated range of test conditions as described in Ref. 10.

Data Acquisition

The pressures were sampled simultaneously at 100 kHz and recorded with 12-bit resolution by a DSP Technology data acquisition system. Three channels were connected to the Baratron pressure transducers to obtain pressures in the driver, detonation, and driven tubes. Nine channels collected data from a single pressure transducer in the driver tube, four in the detonation tube and four in the driven tube. In addition to a direct indication of pressures, the readings allowed time-of-flight calculations for obtaining detonation or shock wave propagation speeds. The wave speed provided an important indication of the properties of the detonation wave, primarily that the wave had indeed transitioned to a fully developed Chapman-Jouguet (C-J) wave. In addition, the wave speed was needed for calculating the properties of the flow past the conductivity channel.

The potential between the anode and the 20 probe electrodes, the voltage across the powered electrodes and the current flowing within the conductivity channel were also acquired. Data from eight of the probe electrodes were gathered at 1 MHz per channel to examine if there was high-frequency unsteadiness.

Seed Injection System

The seed system was designed for injecting powdered material as uniformly as possible in the detonation tube. Powdered, anhydrous potassium carbonate, with a particle size of less than 0.850 mm (20 mesh) and 99.9 percent purity, was used. The seed was blown into the detonation tube by the fuel and oxidizer flow through an injector located at 203 mm (0.33 in.) downstream of the double diaphragm. The injector was a section of tubing bent to blow the seed axially downstream. The amount of flow through the injection system could be controlled via two solenoid valves.

Experimental Results

Test Cases

The parametric experiments were categorized into the following three cases:

- *Case 1: Detonation Tube Seeded (DTS)* where the detonation tube was filled with fuel and oxidizer, and the driven tube was filled with air,

- *Case 2: Whole Tube Detonation (WTD)* where the diaphragm between detonation tube and driven tube was removed and the same detonation mixture filled both tubes,
- *Case 3: Driven Tube Seeded (DRS)* where both the detonation and driven tubes were filled with the same mixture but the mixture in the driven tube was also seeded.

For the second and third types of experiments, the seed injection system was modified in order to inject seed into the driven tube as well. Seeding was one percent of potassium by weight in carbonate form.

The test cases are summarized in Table 1. For each pair of detonation mixtures, the total number of experiments and the number of experiments in which C-J velocity was achieved in the study are listed. The number of unseeded experiments is displayed in parentheses. The initial pressures in the driver, detonation and driven tubes are also tabulated. Initial temperature was 298 K for all the experiments.

Table 1. Test Cases

| | Detonation Mixture | No. of Experiments* | | Initial Pressure [atm] | | |
|-----|--|---------------------|-----------|------------------------|-----------|-------|
| | | Total | Detonated | p_4 | p_{100} | p_1 |
| DTS | H ₂ + O ₂ | 10(3) | 8(3) | 193–217 | 2–3 | 0.5–1 |
| | H ₂ + Air | 3(0) | 2(0) | 201–216 | 3 | 1 |
| | C ₃ H ₈ + O ₂ | 10(4) | 9(3) | 189–213 | 2 | 0.1–1 |
| | C ₃ H ₈ + Air | 5(0) | 0(0) | 200–215 | 2–3 | 0.3–1 |
| WTD | H ₂ + O ₂ | 2(1) | 1(1) | 201–203 | 1 | 1 |
| | H ₂ + Air | 2(1) | 2(1) | 208–209 | 1 | 1 |
| DRS | H ₂ + O ₂ | 3(0) | 3(0) | 202–204 | 3 | 1 |

*(): Unseeded cases

The ideal wave process in the detonation shock tube is shown in Fig. 1(b). When the double diaphragm was ruptured, the high-pressure gas at the initial state 4 expanded into the low pressure section 100, filled with the detonable mixture. A detonation wave was established and proceeded into the driver tube. However, if the driving shock was weaker than that required for the perfectly driven condition, a Taylor rarefaction followed and resulted in a uniform pressure region noted as 400.¹² Assuming isentropic expansion and a calorically perfect gas, the theoretical pressure of this region, can be expressed as

$$(p_{400})^{f(1)} + A(p_{400})^{f(CJ)} + B = 0 \quad (1)$$

where

$$A = \frac{a_{CJ} g_1 - 1}{a_1 g_{CJ} - 1} \left(\frac{1}{p_{CJ}} \right)^{f(CJ)} \cdot (p_1)^{f(1)}$$

$$B = \left[\frac{g_1 - 1}{2} \frac{u_{CJ}}{a_1} - \frac{a_{CJ} g_1 - 1}{a_1 g_{CJ} - 1} - 1 \right] \cdot (p_1)^{f(1)}$$

$$f(i) = \frac{g_i - 1}{2g_i}$$

Equation (1) is not explicit, but from the C-J and initial driver conditions, the plateau pressure of region 400 is known. For a driver gas with a low molecular weight, such as helium or hydrogen, p_{400} becomes large.

The detonation shock was reflected due to the cross-sectional area change and the presence of another diaphragm between the detonation and driven tubes. Chapman-Jouguet conditions were achieved after the reflection. However, due to the progressive attenuation by the Taylor rarefaction, the shock accelerated until it was sufficient to balance the pressure of the expanding driver gas. Also, the detonated mixture proceeding into the driven tube induced another shock, depending on the initial conditions in the detonation and driven tubes. When the detonation tube was seeded (Case 1), seed was found in the regions between the driver interface and the contact surface (100, 200, 400, 500, the expansion wave and 3 of Fig. 1b). In Case (3), seed was in regions 1 and 2, downstream of the contact surface.

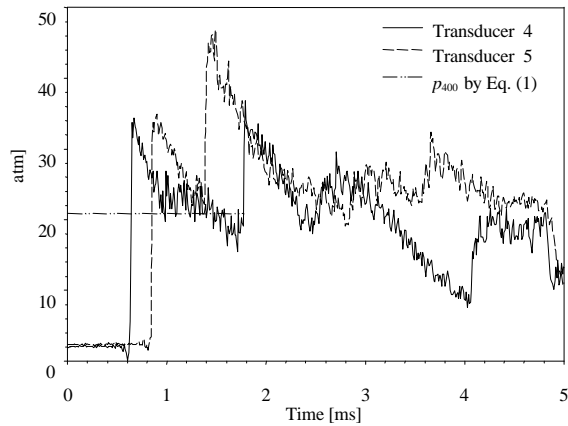


Figure 2. Example of Case (1): pressures in detonation tube. Transducers 4 and 5 are 1.66 m and 2.25 m from the downstream face of the double diaphragm. The first peak is the incident detonation wave. It is followed by Taylor rarefaction and the second peak is the reflected detonation wave.

An example of Case (1) in which an oxyhydrogen mixture is seeded with potassium will be discussed. Figure 2 shows pressures measured in the detonation tube. The detonation wave speed was calculated using a time-of-flight analysis of the propagating detonation wave. From the speed and the distance between the transducers and double diaphragm, the instant that the double diaphragm broke was estimated. The abscissa in Fig. 2 is the time after the diaphragm was ruptured. The

subsequent pressure rise was due to wave reflection. With the known initial conditions, the times when the driver gas arrived at transducers 4 and 5 were calculated as 3.52 and 4.88 ms, respectively. Using Eq. (1), p_{400} was calculated as 20.93 atm. It is hard to determine the plateau pressure in Fig. 2 since the Taylor rarefaction did not fully develop and was terminated by the reflected shock. However, it can be noticed that the experimental p_{400} was slightly lower than the pressure given by Eq. (1).

The pressures recorded in the driven tube are shown in Fig. 3. The abscissa is also referred to the estimated time of diaphragm rupture. The induced velocity in region 2 was supersonic. Thus, the second peak and dip in Fig. 3 were due to another shock and expansion wave behind the primary shock. The expansion wave arrived at transducer 7 around 6 ms and the pressure subsequently decreased.

Further analysis showed several characteristics common to Case (1). First, all the detonations driven by air were under-driven, in which the detonation wave was followed by a Taylor rarefaction wave and the pressure was lower than the C-J pressure. Secondly, the expansion tail in the driver was supersonic. Thirdly, the reflected shock, as seen in Fig. 2, caused the velocity in region 500 to be small or even negative (upstream running) relative to laboratory frame. The induced velocity in the driven tube (region 2 in the wave diagram, Fig. 1b) was supersonic.

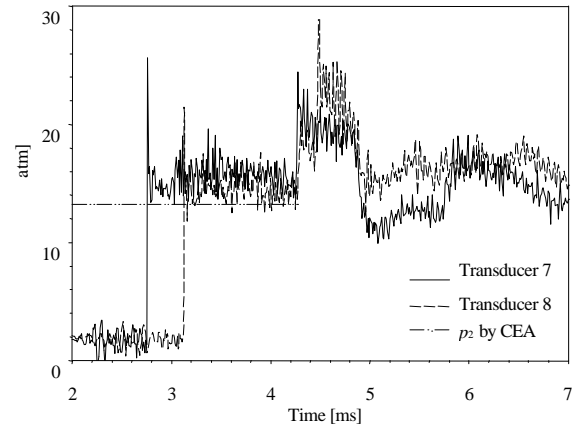


Figure 3. Example of Case (1): pressures in driven tube. Transducers 7 and 8 are 5.32 m and 5.78 m from the downstream face of the double diaphragm.

Figure 4 shows voltage traces measured at the electrical conductivity channel. The top curve is the total applied potential across the powered electrodes. From the tube geometry and shock velocities, the shock passage in the conductivity channel could be tracked. The horizontal bars labeled (a) and (b) indicate respectively the approximate time of passage of the detonation wave and contact surface through the conductivity channel. In

this case, the shock and contact surface passed through the conductivity channel during 3.36–3.47 ms and 4.12–4.26 ms respectively. The flow of the ionized detonation products past the electrodes triggered a current that was detected by an immediate drop in the applied voltage and a rise in the voltage across the 20 probe electrodes, as indicated in the figure.

The measured current is shown in Fig. 5. This figure shows that after transit of the contact surface, the current started to increase. Ohm's law yields

$$s^* = \frac{I/A}{V/L} \quad (2)$$

where I is the measured current, A is the cross-sectional area of the conductivity channel, V/L is the voltage gradient between the first and the last electrodes, and s^* is averaged conductivity. From the data displayed in Fig. 4, it was found that the voltage gradients between adjacent electrodes were constant, which reduces uncertainty in the axial direction. Electrical conductivity averaged over the cross-section is calculated using Eq. (2) and plotted in Fig 5. The figure shows large variations in conductivity before the arrival of the contact surface. This is physically meaningless, since it is due to the negligible voltage gradient across the channel. After the arrival of the contact surface, the figure shows that the conductivity followed the same trend with time as the current trace.

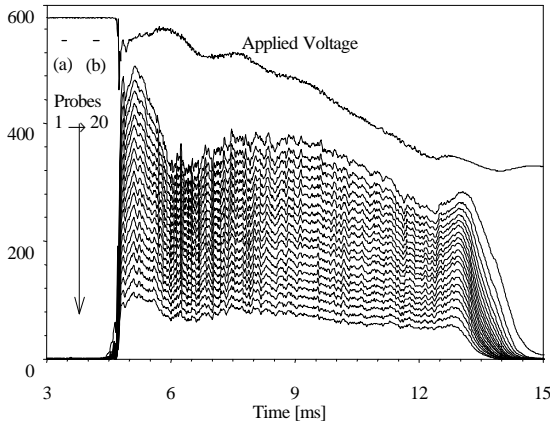


Figure 4. Example of Case (1): voltages across electrodes. Shock and contact surface propagation through the conductivity channel indicated by horizontal bars above (a) and (b), respectively.

The current and conductivity increased after the arrival of the contact surface in the conductivity channel and decreased as the expansion waves passed. Finally as the seeded detonation products fill the channel, current and conductivity increased significantly. The calculated time of driver interface arrival was 13.17–13.45 ms, which is indicated by a decrease of conductivity in Fig. 5.

Most of the experiments in Case (1) displayed features

similar to those discussed above. However, the propane-air mixture did not establish C-J conditions even with the helium driver. Substantial conductivity was also measured in the detonation products from the unseeded mixture. This behavior will be discussed later.

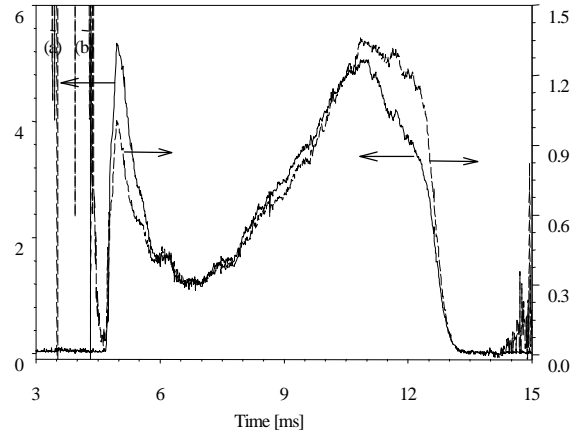


Figure 5. Example of Case (1): measured current and averaged conductivity. Short bars labeled (a) and (b) are same as in Figure 4.

For Cases (2) and (3), detonation also occurred in the driven tube. For Case (2), there was no contact surface since both the detonation and driven tubes were effectively a single detonation tube of constant bore. However, wave reflections in the detonation tube and the arrival of the high-pressure driver gas affected the test flow. Unfortunately, the driven tube and the conductivity channel were not perfectly sealed, requiring that the initial pressure in the conductivity channel to be near atmospheric.

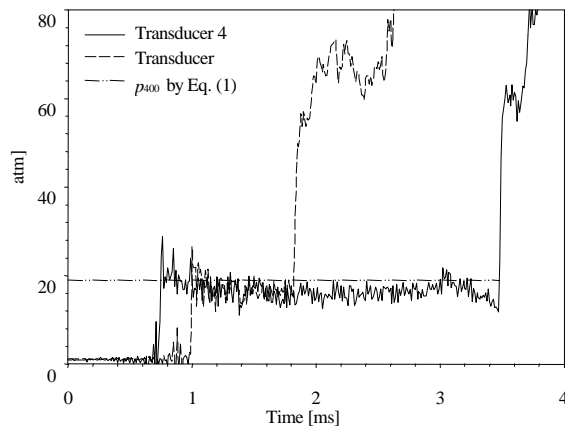


Figure 6. Example of Case (2): pressures in detonation tube. The locations of transducers are same as Figure 2.

Figures 6 and 7 show pressures in the detonation and driven tubes. The detonation mixture was hydrogen and air at 1 atm in both tubes, and the driver gas was helium.

Only slight Taylor rarefaction is indicated in Figs. 6 and 7. The plateau pressure p_{400} is almost the same as the theoretical value of 18.9 atm. Calculations indicated that the driver gas interface arrived at transducer 4 at 1.43 ms when helium was the driver gas (Fig. 6), but arrived at 3.61 ms when air was the driver gas (Fig. 2).

Figures 8 and 9 show the measured electrode voltages, current and averaged conductivity of oxyhydrogen detonation products. The voltage increased immediately after the detonation and dropped after driver gas arrival. The conductivity peaks in Fig. 9 are closer than in Fig. 5 because the use of helium as the driver gas improved shock tube performance. The first peak is due to the conductivity of detonation products within the driven tube while the second peak is due to the arrival of detonation products from the detonation tube.

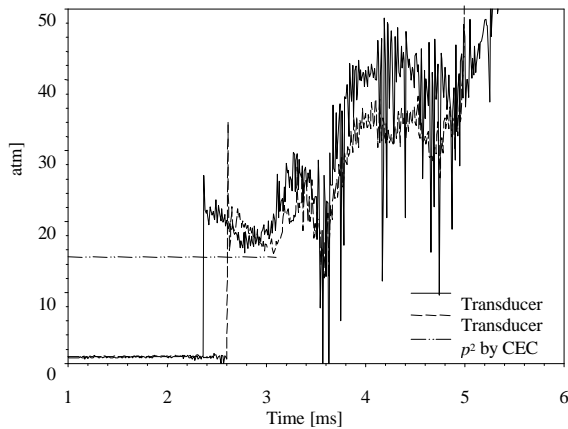


Figure 7. Example of Case (2): pressures in driven tube. The locations of transducers are same as Figure 3.

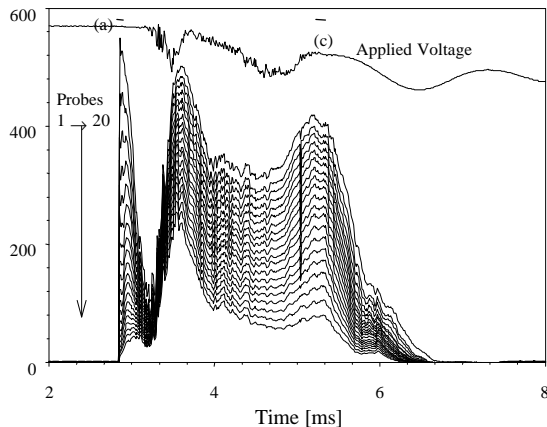


Figure 8. Example of Case (2): voltages across electrodes. Shock and driver gas propagation through the conductivity channel indicated by horizontal bars above (a) and (c).

The general characteristics for Case (3) were similar to Case (2). One notable difference is that the detonated gas in detonation tube was unseeded. The measured conductivity did not show two peaks (Fig. 10). The

conductivity was almost zero before the contact surface arrived. A more detailed description will be provided later.

Analysis

Analysis Overview

Accurate measurement of electrical conductivity of seeded detonation products for PDE exhaust conditions proved to be an extremely difficult task for several reasons. First, the detonation process is strongly dependent on pressure, temperature and the fuel/oxidizer ratio. It is difficult experimentally to obtain an exact and perfect mixture of the reactants. Secondly, the large seed particles used in the present experiments settled inside the tube and created a non-uniform distribution. The large seed size also prevented complete ionization. Moreover, theory indicates that the PDE exhaust temperature was such that small temperature changes could cause large conductivity changes in the seeded flow. Small uncertainties in temperature then resulted in large uncertainty in conductivity. Finally, the theory, which assumes equilibrium conditions, may not model the nonequilibrium processes in practice.

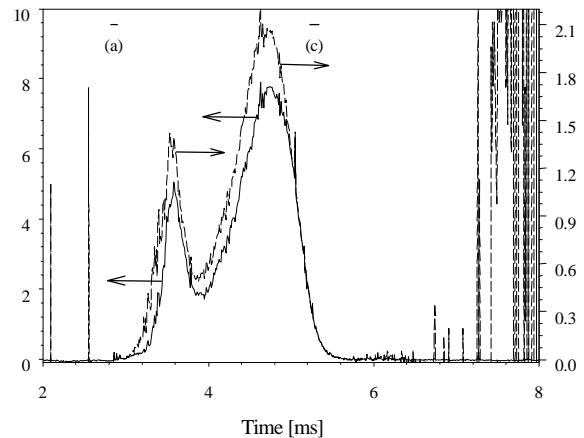


Figure 9. Example of Case (2): averaged conductivity. Short bars labeled (a) and (b) are same as in Figure 8.

An attempt was made to understand the data by assuming that ideal conditions existed. These assumptions include a stoichiometric mixture ratio and complete mixing of the reactants, uniform distribution of seed, and that the detonation can be modeled as a chemically equilibrium process. The data were compared against results generated using CEA.

A wave diagram based on the facility configuration is shown schematically in Fig. 1(b). Given initial conditions in region 100, the C-J velocity and pressure in region 200 (immediately behind the C-J wave) were derived using CEA. Figure 11 shows comparisons of experimental and calculated C-J velocities. The

detonation velocity is strongly dependent on detonation mixture but weakly dependent on initial pressure. The velocities obtained in the experiments are generally lower than their CEA values except hydrogen/air cases. For the hydrogen/air case, incomplete mixing may produce hydrogen/oxygen mixtures locally, resulting in a higher velocity.

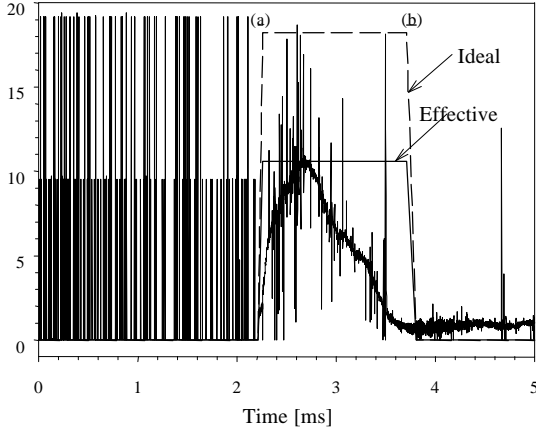


Figure 10. Example of Case (3): Averaged conductivity with effective seed amount: (a) and (b) same as Figure 4. Ideal line represents the conductivity with perfect seed ionization, and line with effective seed is by an equivalent reduced seed.

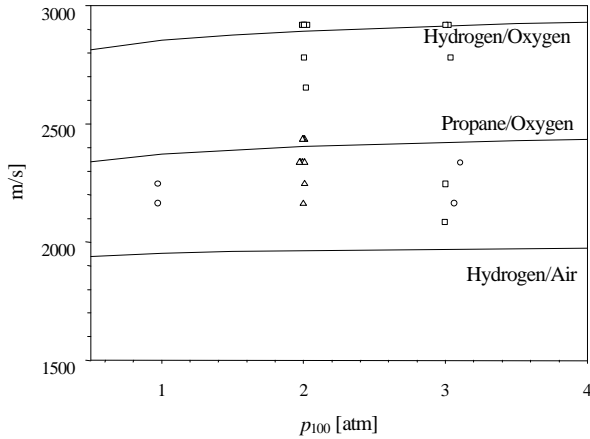


Figure 11. Detonation velocity comparison for mixtures initially at 298 K. CEA results are shown as lines, experimental values for hydrogen/oxygen as squares, for propane/oxygen as triangles, and for hydrogen/air as circles.

Figure 12 compares the measured post-detonation pressure and calculated values obtained using CEA. The experiments and predictions both indicate that the highest pressures were obtained with propane/oxygen mixtures. However, it is difficult to obtain an experimental definition of the C-J pressure p_{CJ} because of the rapid initial decay of the pressure from its peak (von Neumann) value. Nevertheless, the measured value of p_{CJ} can be useful in developing a pulsed MHD device.

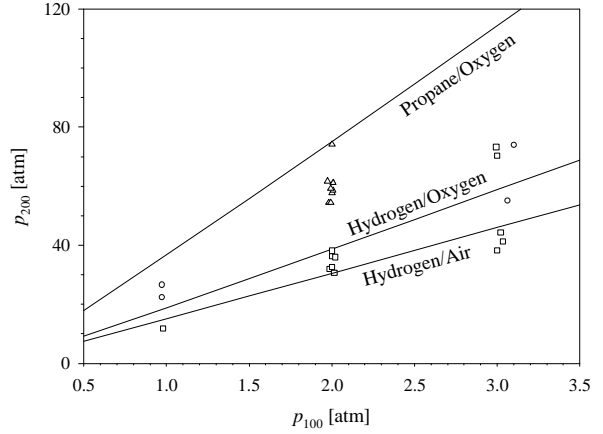


Figure 12. Pressure of detonated products at initial $p = 1$ atm and $T = 298$ K. Symbols as in Figure 11.

The incident detonation wave is partly reflected due to the cross-sectional change between the detonation and driven tubes. Using one-dimensional shock theory and the measured reflected wave speed, the pressure and temperature in region 500, p_{500} and T_{500} were calculated. The pressure and temperature in region 2, p_2 and T_2 were also computed using CEA and the measured shock speed in driven tube. Since the pressures in region 2 and 3 are the same, $p_2 = p_3$, T_3 was derived using the isentropic relation

$$\frac{T_3}{T_{500}} = \left(\frac{p_3}{p_{500}} \right)^{\frac{g_{500} - 1}{g_{500}}} \quad (3)$$

The results are only approximate since the flow through the area reduction between the detonation tube and the driven tube is non-isentropic and T_{500} is not accurately known.

CEA, modified with the Demetriades-Argyropoulos multicomponent isothermal model,¹³ was used to obtain theoretical values of electrical conductivity in the high-pressure plasma. The results are shown in Fig. 13 for detonation products with and without seed at one percent by weight of potassium. The vertical bars indicate the range of theoretical conductivity for the different products from 5 to 30 atm. The figure shows that the predicted electrical conductivity of seeded detonation mixtures is two to three orders of magnitude higher than the unseeded gas. Moreover, electrical conductivity increases dramatically with temperature but decreases with pressure. For unseeded mixtures, the figure shows an extremely rapid drop of conductivity for the unseeded gas when the temperature drops below 3700 K to negligible values. The theoretical results indicate that there may be difficulties in achieving adequate ionization for high-pressure MHD devices even with seed.

The measured conductivities are also plotted in Fig. 13 as a function of temperature T_3 calculated by the method

delineated above. Since the conductivity is strongly dependent on temperature, T_3 must be accurately known, which was not feasible in the present experiments. However, it can be seen that the measured conductivity is lower than predictions. Some reasons for this anomaly will be discussed in the next section.

Discussion

Data Uncertainty

The uncertainty of some key parameters is displayed in Table 2. The initial pressure p_1 was subject to a high degree of uncertainty because the Baratron pressure transducer had to be isolated prior to firing the tunnel to prevent damage resulting from over-pressurization. Small leaks in the conductivity channel caused the pressure to change by an unknown amount between isolation of the transducer and diaphragm rupture. While this did not affect the accuracy, it adversely affected the ability to precisely set the pressure ratio to achieve a desired shock speed. The uncertainty in averaged conductivity was due to the uncertainty in determining the extent of the uniform voltage gradient near the power electrodes.

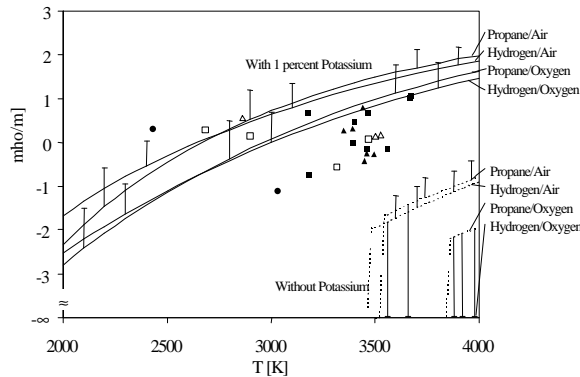


Figure 13. Theoretical and experimental conductivity at $p = 30$ atm. Theoretical results are shown in lines, the experimental values for hydrogen/oxygen as squares, for propane/oxygen as triangles, and for hydrogen/air as circles. Vertical bars show conductivity for pressures down to 5 atm. Open symbols represent unseeded and closed symbols represent seeded mixtures.

Table 2. Data Uncertainties

| | | | |
|-------|--------------|------------|-------------|
| p_1 | $\pm 16.1\%$ | p_2 | $\pm 5.4\%$ |
| T_1 | $\pm 1.0\%$ | T_2 | $\pm 5.5\%$ |
| I | $\pm 1.0\%$ | V | $\pm 1.0\%$ |
| s^* | $\pm 4.6\%$ | m_{seed} | $\pm 1.3\%$ |

Tube Erosion

The data indicated a measurable current in the flow of the unseeded products. It was thought that the conductivity might be due to erosion of the driven tube. It is

known that the melting point of stainless steel 304 is 1400 K. The nominal temperature of region 2 is about 1400 K and the temperature of detonated plasma is higher than 2000 K. Evidence of erosion was found in the coupling between the detonation tube and the driven tube. For the unseeded flow, the maximum current appeared to be unrelated to the temperature. However, the time-averaged current was found to be proportional to the post-detonation temperature T_2 , as shown in Fig. 14. (The averaging was done up to the arrival of the expansion wave.)

The effect of tube erosion appeared to be more severe in propane/oxygen mixtures than hydrogen/oxygen mixtures. The effect in hydrogen/air mixtures was intermediate. It therefore appears that the erosion was not only caused by high temperature but its severity depends on the composition of the reactants.

Non-Uniform Seeding

Potassium carbonate in a finely powdered form was injected with the fuel into either the detonation or the driven tube. To achieve maximum conductivity, the seed should be uniformly distributed through the tube and be suspended in the reactants to provide a homogeneous mixture at the initiation of the detonation. However, a uniform axial distribution and a homogeneous mixture were each difficult to achieve. A nonuniform distribution occurred when the single point seed injector blew more seed into one portion of the tube than into another; a vertically non-homogeneous mixture may also occur due to settling of the particles after filling and prior to detonation.

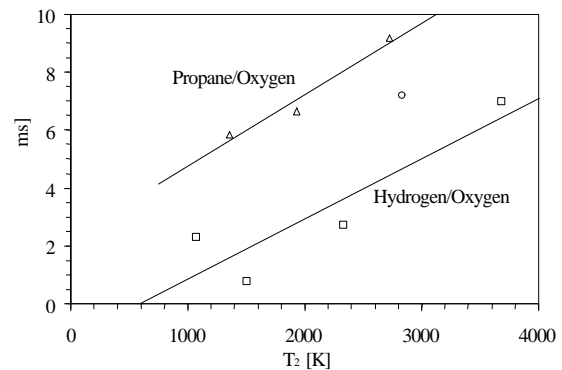


Figure 14. Integrated current of unseeded detonation gas. The linear regressions with T_2 are shown as lines, the experimental values for hydrogen/oxygen as squares, for propane/oxygen as triangles and for hydrogen/air as circles.

Filling and post-filling procedures required 20 to 25 minutes for completion. Significant seed settling can occur during this period unless the seed is grounded to an extremely fine powder. A simplified analytical approach was used to estimate the seed settling rates as a function of particle size.

The rate of settling of potassium carbonate seed parti-

cles in the detonation mixture prior to detonation can be estimated by calculating the terminal velocity of the particles.¹⁴ Assuming the particles to be spherical and equating the drag force to the particle weight gives an expression for velocity as

$$u_t = \sqrt{\frac{4gD_p(\mathbf{r}_p - \mathbf{r})}{3rC_d}} \quad (4)$$

where D_p is the diameter of the particle, C_d is the drag coefficient, \mathbf{r}_p is the density of the particle and \mathbf{r} is the density of the reactant mixture. The drag coefficient C_d of spherical particles for the range of Reynolds numbers (based on diameter) encountered is given by

$$C_d = \frac{24}{Re} \quad \text{for } Re < 0.3 \quad (5)$$

$$C_d = \frac{18.5}{Re^{0.6}} \quad \text{for } 0.3 < Re < 10^3 \quad (6)$$

Assuming that particles continuously fall at the constant terminal velocity, the settling distance during one minute for 20 mesh was as much as 250 m. (1500–2000 tube diameters). The seed with diameters in the 4–5 mm range would settle approximately one tube diameter during one minute. Submicron particles are needed if they are to remain suspended in a nearly homogeneous mixture during delays of several minutes before detonation. Such particles will be extremely difficult to obtain.

Effective Seed

Case (3) provided indication that the seed was not vaporized by the detonation wave. Since seed was injected only in the driven tube, conductivity should be measured only in region 2 of the wave diagram. In other words, ideally, conductivity increases as the detonation wave enters into conductivity channel and decreases as the contact surface leaves from conductivity channel. For oxyhydrogen at $p_1 = 1$ atm and $T_1 = 298$ K, the ideal conductivity is shown in Fig. 10. However, the measured conductivity did not reach that theoretical level. Instead, the measured conductivity started to increase gradually and then decreased. This is thought to be due to the relatively slow evaporation of seed. To further comprehend the effect of seed evaporation, the ratio of integrated conductivity to integrated ideal conductivity was calculated as 33.5 percent. This conductivity due to an “effective seed” is shown in Fig. 10. In general, the experiments indicated that the evaporation rate was 30 to 40 percent.

Figure 10 indicates that the maximum value of the experimental conductivity coincided with the calculated conductivity with a reduced amount of seed. In this analysis, the effects of seed settlement and tube erosion were not considered. If these effects were included, the effective seed amount will be smaller.

Incomplete Mixing

As shown in Table 1, in some experiments, the C-J detonation velocity could not be achieved. Also as seen in Figs. 11 and 12, the detonation velocity and pressure were found to deviate from theoretical values. The effect of incomplete mixing of fuel and oxidizer on the wave speed and pressure was explored analytically in this section as a possible cause for this deviation. An approximate model of incompletely mixed fuel and oxidizer was used to simulate the conditions and evaluate the possibility that this might cause the reduced detonation performance.

Equilibrium analyses were performed by substituting non-reactive helium for a fraction of the hydrogen in the reactants to simulate incomplete mixing in the detonation tube. Helium was used in this analysis, since its low molecular weight would not significantly change the mixture average molecular weight from that of the stoichiometric oxyhydrogen mixture. The C-J detonation routine in CEA was used to assess the effect. A comparison of the theoretical detonation pressure and velocity with the experimentally measured values in Fig. 15 indicates that the experimental values can be closely matched with the theoretical results using 60 percent reactive hydrogen.

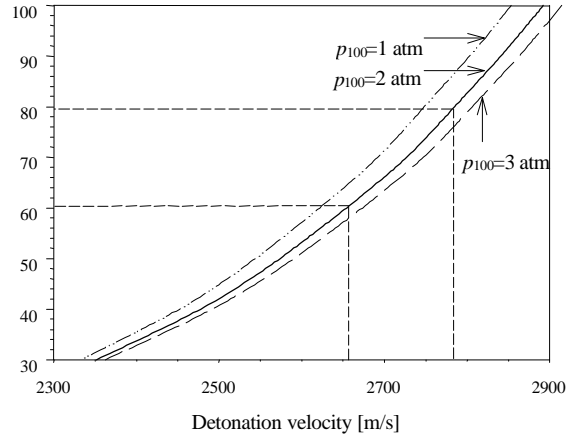


Figure 15. Incomplete mixing effect on detonation velocity in hydrogen/oxygen mixture. Drop lines show experimental values.

To test the validity of this approach, another set of chemical calculations was made with substitution of inert gases to simulate nonreactive oxygen instead of hydrogen. For this calculation, a mixture of 60 percent argon and 40 percent neon was used to produce approximately the same average molecular weight as molecular oxygen (32 kg/kmol). Again, the best fit was found when more than 60 percent of the hydrogen was reactive. With this percentage, both pressure and velocity were well matched to within the estimated experimental error.

Hydrogen and oxygen are difficult to mix due to their large molecular weight difference and require dynamic

mixing during injection or long settling times when injected separately in order to obtain a homogeneous mixture. However, long settling times were not practical for these experiments, since powdered seed was introduced with the fuel during filling, and the entire seed would settle to the bottom of the tube if the detonation was not initiated immediately after tube filling was completed. Some experimentalists have recommended that the tube be allowed to sit for hours before detonation. However, due to the operational requirements, such as leaking or seed settling, the mixture were detonated after only a few minutes. Thus, the findings of this analysis are consistent with anecdotal evidence concerning the slowness in mixing of hydrogen/oxygen system.

Conclusions and Recommendations

Detonations were achieved in hydrogen/oxidizer and propane/oxygen mixtures. However, propane/air mixtures could not sustain a C-J detonation within the facility. The experiments obtained measurable conductivity in the detonation products. However, the measured conductivity was substantially lower than theoretical values using CEA. It was thought that poor seed distribution and incomplete vaporization might be causes for the low values of measured conductivity. Moreover, the measurements indicated that unseeded gas also had comparable conductivity. This anomalous result may be due to contamination by steel particles eroding from the driven tube.

Despite the difficulties encountered in the experiments, this study allowed several conclusions to be derived. The major difficulty in realizing mixtures with high conductivity in experimental tests is the seed injection and distribution. A better design will be implemented in the future, particularly for implementation with a pulsed detonation engine.

Acknowledgements

Funding for this study was provided by MSE-TA, Inc., Butte, Montana.

References

- ¹ Back, L. H., Dowler, W. L., and Varsi, G., "Detonation Propulsion Experiments and Theory," *AIAA Journal*, Vol. 21, No. 10, 1983, pp 1418–1427.
- ² Bird, G. A., "A Note on Combustion Driven Shock Tubes," in "Hypersonic Facilities in the Aerodynamics Department, Royal Aircraft Establishment," edited by P. A. Hufton, AGARD Report 146, 1957.
- ³ Lu, F. K., Wilson, D. R., Stuessy, W. S., Bakos, R. J., and Erdos, J. I., "Recent Advances in Detonation Techniques for High-Enthalpy Facilities," AIAA Paper 98-0550, 1998.
- ⁴ Lee, B. H. K., "Detonation-Driven Shocks in a Shock Tube," *AIAA Journal*, Vol. 5, No. 4, 1967, pp. 791–792.

- ⁵ Garrison, G. W., "Electrical Conductivity of a Seeded Nitrogen Plasmas," *AIAA Journal*, Vol. 6, No. 7, 1968, pp. 1264–1270.

- ⁶ Unkel, W., and Freeman, A., "Conductivity Measurements of Phosphorous-Doped Potassium-Seeded MHD Plasmas," *AIAA Journal*, Vol. 21, No.12, 1983, pp. 1648–1651.

- ⁷ Lu, F. K., Wilson, D. R., Liu, H-C., and Stuessy, W. S., "Experiments on Weakly-Ionized Air and Nitrogen Plasmas for Hypersonic Propulsion Facility Development," abstract submitted to the 35th AIAA/ASME/SAE/ ASEE Joint Propulsion Conference and Exhibit, Los Angeles, California, June 20–24, 1999.

- ⁸ Gordon, S., McBride, B.J., "Computer Program for Calculation of Complex Chemical Equilibrium Composition, Rocket Performance, Incident and Reflected Shocks, and Chapman-Jouguet Detonations," NASA SP-273, 1976.

- ⁹ Stuessy, W. S., Liu, H.-C., Lu, F. K., and Wilson, D. R., "Initial Operation of a High-Pressure Detonation-Driven Shock Tube Facility," AIAA Paper 97 0665, 1997.

- ¹⁰ Liu, H.-C., Stuessy, W. S., Lu, F. K., and Wilson, D. R., "Design of an Electrical Conductivity Channel for Shock Tunnel," AIAA Paper 96-2198, 1996.

- ¹¹ Adler, R. J., *Pulse Power Formulary*, North Star Research Corporation, Albuquerque, New Mexico, 1989.

- ¹² Bakos, R. J., Castrogiovanni, A., Calleja, J. F., Nucci, L., and Erdos, J. I., "Expansion of the Scramjet Ground Test Envelope of the HYPULSE Facility," AIAA Paper 97-4506, 1996.

- ¹³ Demetriades, S. T. and Argyropoulos, G. S., "Ohm's Law in Multicomponent Nonisothermal Plasmas with Temperature and Pressure Gradients," *Physics of Fluids*, Vol. 8, No. 11, 1966, pp. 2136–2149.

- ¹⁴ Perry, R. H. and Chilton, C. H., *Chemical Engineers' Handbook*, 5th edition, McGraw-Hill, New York, 1973.